+SPEA introduction: drastic actuator energy requirement reduction by symbiosis of parallel motors, springs and locking mechanisms

Mathijssen, Glenn; Furnémont, Raphaël; Verstraten, Tom; Brackx, Branko; Premec, Jasmina; Jimenez Fabian, Rene Enrique; Lefeber, Dirk; Vanderborght, Bram

Published in:
IEEE International Conference on Robotics and Automation (ICRA)

DOI:
10.1109/ICRA.2016.7487193

Publication date:
2016

Document Version:
Accepted author manuscript

+SPEA introduction: drastic actuator energy requirement reduction by symbiosis of parallel motors, springs and locking mechanisms

Glenn Mathijssen[1,2*o], Raphaël Furnémont[1*], Tom Verstraten[1], Branko Brackx[1], Jasmina Premec[1], René Jiménez[1], Dirk Lefeber[1], and Bram Vanderborght[1]

***Abstract*— Modern actuation schematics become increasingly ingenious by deploying springs and locking mechanisms in series and/or parallel. Many of these solutions are, however, tailored for a specific application and a general schematic that allows for drastic energy reduction remains a challenge. We have developed a series-parallel elastic actuator (SPEA) based on a symbiosis of multiple motors, springs and locking mechanisms in parallel, which we call +SPEA. This paper introduces the novel +SPEA concept. We present a first prototype, a +SPEA model and a control strategy that optimizes the energy consumption, and experiments to verify the working principle and recruitment strategy. The experiments show a good fit with the model and currently the actuator reduces the required energy in blocked output experiments by more than a factor 4.**

I. INTRODUCTION

One reason compliant actuators received increasing attention in the robotics research community over the years is the ability to store and release energy. The two well known actuation schematics are the series elastic actuator (SEA) [1] [2], where a spring is placed in series with a servo motor, and the parallel elastic actuator (PEA) [3] [4] where a spring is placed in parallel with a servo motor. The schematics allow to, respectively, alter the speed and torque trajectory of the motor in comparison to stiff actuators. A combination of both, often referred to as SE+PEA, can alter both the speed and torque trajectories [5]. However, the versatility of these compliant actuators is limited since the alteration of the speed or torque profile is pre-defined by the actuator architecture itself.

In more recent years, several compliant actuators have been developed that incorporate clutches. The clutches enable to switch between different actuation schematics, as a function of the actuation phase or application [6]. A recent review on locking devices in robotics can be found in [7]. One example is the clutchable series-elastic actuator presented in [8], which can switch from an SEA to a pure passive spring. Another example is the clutched parallel elastic actuation concept presented in [9], which can switch from stiff actuator to PEA. The knee actuator from [10] consists of a SEA drive with a parallel spring which can be driven by an additional motor or locked by a locking mechanism.

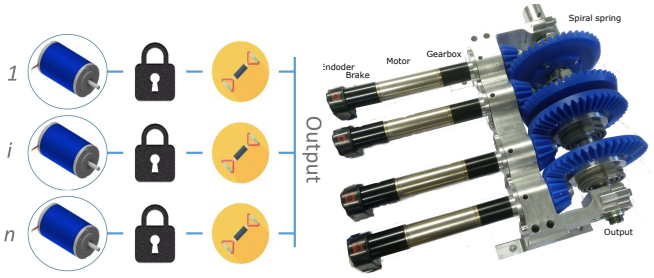

(a) +SPEA schematic (b) +SPEA prototype

Fig. 1. Each motor unit in the +SPEA schematic (a) consists of a motor, a locking mechanism and a spring. The +SPEA prototype (b) presented in this work consists of 4 parallel motor units and is shown in the picture. Each component of one of these units, together with the essential actuator components, are highlighted.

In summary, one could say the above examples all deploy springs in the actuation schematic, whether or not clutchable, in order to optimize either the motor torque profile, speed profile, peak power, peak torque, energy consumption or similar. The single motor is then controlled for a specific task, such as position or force tracking. The novelty in this work is the symbiosis of multiple parallel motor units, consisting of a SEA with locking mechanism, driving a single output. This redundancy can be exploited in order to, for example, minimize energy requirements. The addition of a locking mechanism, whether passive or active, is crucial in each motor unit to be to able relieve the motor from holding torque. We call this novel actuation schematic plus series-parallel elastic actuation (+SPEA). The essential components are indicated in the schematic in Fig. 1a, and a picture of the first +SPEA prototype is shown in Fig. 1b.

In Section II we first discuss our previous SPEA work and clearly indicate the difference with the work presented in this contribution. The novel +SPEA prototype is presented in Section III. Next, the model and control strategy of the +SPEA are introduced and discussed respectively in Section IV and V. Finally, the experiment described in Section VI verifies the claimed energy reduction by variably canceling load by means op deploying multiple springs, motors and locking mechanisms in parallel in one joint.

II. FROM ıSPEA TO +SPEA

The work on the +SPEA fits into our prior SPEA work. In this Section II we would like to differentiate from, and

* The first two authors contributed equally to this work and should both be considered as first author.

[1] Robotics & Multibody Mechanics Research Group, Faculty of Mechanical Engineering, Vrije Universiteit Brussel, 1050 Brussels, Belgium. http://mech.vub.ac.be/robotics

[2] Interdepartemental Research Centre E. Piaggio, Faculty of Engineering, University of Pisa. http://www.centropiaggio.unipi.it/

[o] Corresponding author: glenn.mathijssen@vub.ac.be

compare with our prior work.

A. iSPEA: SPEA with intermittent mechanism

In prior work we introduced the SPEA concept [11], which enables variable recruitment of n parallel springs and variable load cancellation. Different mechanical solutions are possible and can be named as dephased intermittent mechanisms that enable, a relatively small, motor to tension and lock different parallel springs in succession. As confirmed in [12] the maximum motor torque can be be approximately lowered by n compared to an equivalent SEA. The energy requirements can be drastically lowered as well (up to an order of magnitude). We name these prior works intermittent series parallel elastic actuation (iSPEA), referring to the intermittent mechanism.

B. +SPEA: SPEA based on a symbiosis of multiple motors, springs and locking mechanism in parallel

It is important to note that since only one motor is available in an iSPEA, load can be canceled variably, but not optimized since each spring needs to be recruited in succession by the intermittent mechanism. The novel +SPEA presented here has the potential to drastically lower actuator energy requirements on two levels:

- The locking mechanism in each motor unit enables to deliver part of the output torque, while the motor can be locked, the motor power is 0 W, without locking the +SPEA output itself.
- The motors in parallel create a redundant system, so that an optimal solution can be found to, for example, let as many motors and gearboxes work at their highest efficiency point. This means, inefficient motor operation at low speeds and/or low torques can be avoided, and gearboxes can be used in the upper half of their torque range where the efficiency is typically the highest.

In this contribution we focus on studying the potential of the former. In previous work [13] we developed actuation modules that consist of multiple motor units in series and parallel, and which can be connected in various combinations themselves. Although the discrete recruitment of these units is still an interesting study topic, the difference with the +SPEA work presented here is that a locking mechanism is added in each motor unit.

III. MECHANICAL DESIGN +SPEA

The +SPEA presented in this paper consists of 4 identical motor units in parallel. Each motor unit consists of: an encoder, a brake, a motor, a gearbox, a last gear stage (i.e. a bevel gear), and a spiral spring which is then finally connected to the output shaft. In this Section III the component selection will be first discussed, followed by the actuator overview and specifications. Finally, the test set-up used in this paper is described.

A. Component selection

The basis of each motor unit is identical:

- Encoder HEDL (ref. 110512): 500 CPT.
- Brake (ref. 301212): 24 VDC and 0.1 Nm.
- Maxon EC motor - 4 pole 22 (ref. 311536): 120 W and 0.0649 Nm nominal torque.
- Gear GP22 HP (ref. 370784): 109:1 and 3.5 Nm max. cont. output torque.

Each Maxon motor is in line with a last bevel gear stage with a 3:1 gear ratio, leveraging the total gear ratio to 327:1 and the maximum continuous torque of the drive to approximately 10 Nm. The bevel gear and pinion are made of Nylatron® MC901, which makes them strong enough to cope with the fraction of the output torque delivered by that motor unit, though lightweight. Each motor train is equipped with a custom laser-cut spiral spring in series. A standard spring steel was selected: 1.4310 Chromium-nickel austenitic stainless steel (AISI 301). The springs were produced by Raytech (Brugge, Belgium). The production process yields a good quality up to 0.003 m. The spring parameters in order to obtain a spring that produces 3.125 Nm at 50^o of deflection, results in the following spring parameters (including a safety factor of 1.3):

- t = 0.0028 m (section thickness)
- L = 0.277 m (unwrapped spring length)
- m = 0.018 kg
- d_o = 0.045 m (output diameter)

When combining 4 springs, with the above characteristics, in parallel; the theoretical spring stiffness becomes 14.32 Nm/rad (i.e. a maximum torque 12.5 Nm at 50^o). The outer diameter of the springs is fixed to the bevel gear, while the inside is fixed to the output shaft in order to transmit the torque produced by each motor unit to the output.

B. Actuator overview and specifications

The Maxon holding brakes provide a convenient and lightweight solution for incorporating the locking mechanism. The brakes are closed by default (by internal springs) and can be unlocked when activated with 24 V. One disadvantage is the fact that these brakes cannot perform dynamic braking, since the generated heat cannot be dissipated. As such, the motors need to be controlled to a standstill before the holding brake can be enabled.

The spiral springs did not undergo any heat treatment after the laser cutting process, which results in remaining internal stresses. Although the hysteresis and linearity of the spiral springs are good, the spring stiffness is lower than modeled. The measured spring stiffness of 4 springs in parallel was apprixamately 8.4 Nm/rad. Therefore, the maximum actuator output torque is currently equal to 25 Nm. With a revised spring version, this can be increased to 40 Nm.

In order to allow the +SPEA to execute tasks for applications such as prostheses and co-workers, a torque bandwidth of 1 Hz in nominal operation is set as a requirement. With a gear ratio of 330:1, it is calculated that the +SPEA actuator can maximally deliver 11.4 Nm at 1 Hz torque bandwidth

(considering the maximum spring deflection at 50^o). The actual gear ratio of 327:1 ensures a torque bandwidth close to 1 Hz.

C. Test set-up

The Maxon motor in each motor unit is driven by a commercial motor drive (ESCON 50/5 250 W, *Maxon motor*). The motor drives are configured to provide real-time information about the actual current and velocity of the motors through their dedicated analog outputs and to process the motor encoder measurements for velocity regulation. The motor voltage is deducted through the current and velocity readings, via the motor model.

The actuator tests were performed attaching the +SPEA, as it is shown in Fig. 2. The output link is connected to the reference frame through a torque sensor (DRBK-200 200 N, *ETH messtechnik*) that allows the direct measurement of the actual actuator's output torque.

The signals from all the sensors and those provided by the motor drives are captured by a real-time data-acquisition (DAQ) system implemented with multifunction input/output boards (PCI-6602 for the encoder readings and PCI-6229 for the analog input-outputs and digital outputs, *National Instruments*). The DAQ boards are installed on a PC (Core™2 CPU 6600 at 2.40 GHz, *Intel*) running Real-Time Windows Target® and Simulink®. This system also allows the implementation of conventional proportional controllers for the angular position of the motors and off-line data processing. The motors were controlled by the commercial drives using external reference inputs also generated by the DAQ system. The full system was powered by regulated industrial power supplies (CP-E 24.0 V / 20 A, CP-E 48.0 V / 10 A, *ABB*).

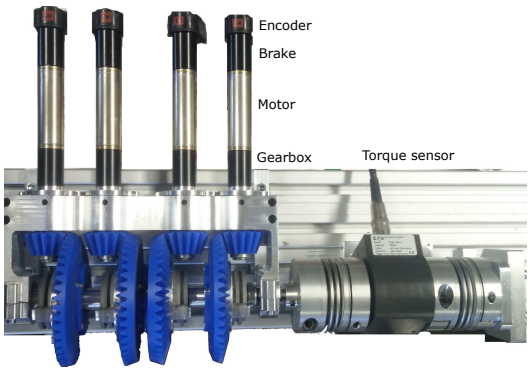

Fig. 2. The torque sensor is connected to the +SPEA output on one side, and blocked to the frame on the other side.

IV. Model of the +SPEA

The +SPEA is thus composed of several Series Elastic Actuators (p denote the amount of SEAs), with the same design, placed in parallel and connected the output axis. Fig. 3 depicts the schematic of the +SPEA. θ_{mi} and T_{li} (i is the index of the unit considered) are the positions of the motors and the loads on the axes of the motors respectively. The positions of the motors and the loads are denoted by, after reduction of the gearboxes, θ_i and T_i. Finally compliant elements of stiffness K are placed between the output, whose position is given by θ_o, and the gearboxes of each motor. The total torque exerted on the output axis is T_o. Holding brakes are placed on each motor. As mentioned in section III-A the brakes are closed by default and thus a voltage U_{bi} =24V needs to be applied in order to use a motor. One can notice that when the brake of a motor is closed the motor does not consume any current/energy and the compliant element acts as a parallel spring which holds a certain torque. The brakes consume power but this consumption is not considered in the model since in time the brakes will be replaced by passive non-backdrivable mechanisms.

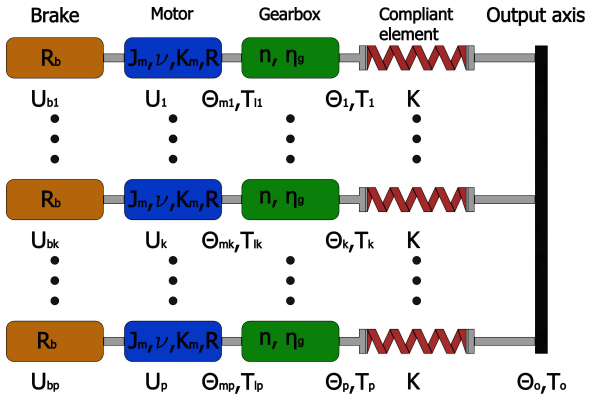

Fig. 3. Schematic of the +SPEA. J_m is the inertia of the rotor, ν is the friction coefficient of the motor, K_m is the torque/speed constant of the motor and R the resistor of the rotor while R_b is the resistance of the coils of the brakes (the power consumed by the brakes being U_{bi}^2/R_b). n and η_G are the transmission ratio and the maximum efficiency of the gearboxes.

First the model of the DC motors (with neglected inductance) is given [14]:

$$\begin{cases} J_m\ddot{\theta}_m + \nu\dot{\theta}_m = K_m I - T_l \\ RI = U - K_m\dot{\theta}_m \end{cases} \quad (1)$$

In equation (1) θ_m is the position vector of the different motors $\left(\theta_m = \begin{pmatrix} \theta_{m1} & \dots & \theta_{mp} \end{pmatrix}' \right)$. I, T_l and U are also vectors with the currents, loads and voltages of the different motors. Next comes the transmission (gearbox):

$$\begin{cases} T_l = \frac{C_G T}{n} \\ \dot{\theta}_m = n\dot{\theta} \end{cases} \quad \begin{cases} C_{Gi} = \frac{1}{\eta_G} \quad if \quad T_i\dot{\theta}_i \geq 0 \\ \qquad = \eta_G \qquad\quad T_i\dot{\theta}_i < 0 \end{cases} \quad (2)$$

C_{Gi} is the efficiency of the gearbox and takes two different values depending on whether the load is driving the DC motor (generator) or if the DC motor is driving the load (motor). Then comes the compliant elements:

$$\begin{cases} T = K(\theta - 1_{p*1}\theta_o) \\ \sum_{i=1}^{p} K(\theta_i - \theta_o) = 1_{1*p}.K(\theta - 1_{p*1}\theta_o) = T_o \end{cases} \quad (3)$$

1_{p*1} and 1_{1*p} is simply vectors of size p*1/1*p filled with ones. K is the stiffness of the springs and the second line of equation (3) indicates that the sum of the torques of all the units is equal to the output torque. The last part to detail

are the brakes. As mentioned holding brakes can only hold the torque of the motors when they are stopped. This implies that the brake of a motor can only be used when the velocity of the motor is zero (hence $\dot{\theta}_{mi} = 0$). To represent how the brakes work a function $D(x)$ will be defined:

$$D(x) = \begin{cases} 1 & \text{if} \quad x = 0 \\ 0 & \text{otherwise} \end{cases} \tag{4}$$

The load on a DC motor T_{li} will be replaced by $T_{lbi} = T_{li}(1 - D(\dot{\theta}_i U_b))$. If the motor k is still and no voltage is applied on its brake $D(\dot{\theta}_k U_{bk}) = 1$ and $T_{lbk} = 0$. As a result, the motor should not consume any power as the load, velocity and acceleration are zero. In any other case $D(\dot{\theta}_k U_{bk}) = 0$ and $T_{lbi} = T_{li}$ showing that the brake has no influence on the behavior of the system. The whole system can be summarized as follow:

$$\begin{cases} J_m \ddot{\theta}_m + \left(\nu + \frac{K_m^2}{R}\right)\dot{\theta}_m = \frac{K_m}{R} U - T_{lb} \\ T_{lbi} = \frac{C_{Gi}}{n} K \left(\frac{\theta_{mi}}{n} - \theta_o\right)\left(1 - D\left(\dot{\theta}_i U_{bi}\right)\right) \\ 1_{1*p}.K(\theta_m/n - 1_{p*1}\theta_o) = T_o \\ P_i = U_i I_i \end{cases} \tag{5}$$

The important variables and parameters of the model present in equation (5) are given in table I:

J_m	rotor inertia of the motor	ν	motor friction coefficient
K_m	motor speed/torque constant	R	resistor of the motor
n	transmission ratio	η_G	transmission efficiency
K	spring stiffness	θ_m	motor position
U	motor voltage	I	motor current
θ_o	output position	T_o	output torque

TABLE I

VARIABLES AND PARAMETERS OF THE +SPEA

V. CONTROL STRATEGY OF +SPEA

The system used has 8 (2p) variables (the voltages on the DC motors U and the voltages on the brakes U_b) for one joint. Due to this redundancy it is possible to achieve extra objectives. In this case the goal was to reduce the energy consumption of the actuator for a given task. Once a brake is used the unit acts as a parallel spring. Finding an optimal control strategy for the system presented in equation (5) was not possible currently because of difficulty with the discontinuous function $D(x)$ and thus an alternative strategy was defined. This approach consists on splitting the optimization in two parts.

First an optimization defining when to use the brakes and how (thus defining the voltages U_b), is defined. Then, a second optimization to find the optimal controls for the DC motors (hence the voltages U) is performed. The optimization used for the brakes is detailed in section V-A while the optimization of the DC motors is described in section V-B.

A. Control strategy of the brakes

As mentioned in section V, a unit acts as a parallel spring when its brake is on. The difference with a PEA is that it is possible to set the equilibrium angle of the parallel spring. There are four variables defined: the braking angles $\theta_{mb}(t)$ (expressed before the gearbox), the amount of motors braking $b(t)$, the time when the motors start to brake $t_{1,j}$ and the times at which they stop $t_{2,j}$ (j is an index to distinguish the different braking motor units). The first optimization defines these four variables, based on a given task $(T_o(t), \theta_o(t))$, with the objective to reduce the load of the non braking motors (J_1):

$$\begin{cases} J_1 = \int_{t_0}^{t_f} \left(T_o - b(t)K\left(\theta_{mb}(t)/n - \theta_o(t)\right)\right)^2 dt & \\ |\theta_{mb}(t)/n - \theta_o(t)| \leq \sigma_{max} & \forall t \in [t_{1,j}; t_{2,j}] \\ |T_o - b(t)K\left(\theta_{mb}(t)/n - \theta_o(t)\right)| \leq b(t)K\sigma_{max} & \forall t \in [t_{1,j}; t_{2,j}] \\ t_{2,j} \geq t_{1,j} + \Delta t_a & \forall j \\ t_{1,j+1} \geq t_{2,j} + \Delta t_r & \forall j \end{cases} \tag{6}$$

There are four inequality constraints. The first one ensures that the springs that are locked do not undergo plastic deformation (σ_{max} is the maximum deformation the springs can undergo). The second constraint ensures that the motors that are not braking can still provide the remaining required torque at the output. The optimization was done brute force and two additional constraints were added to reduce the computation time: a minimum activation time Δt_a during which the brakes are used and a minimum resting time Δt_r during which the brakes are not used. One can notice that this optimization does not aim to reduce the consumption of the motors (their characteristics is not even accounted) but goes into that direction as the Joule losses are proportional to the load carried by the motors. Additionally the motors braking are all doing it at the same time and at the same angles. The results of the optimization are shown on Fig. 4.

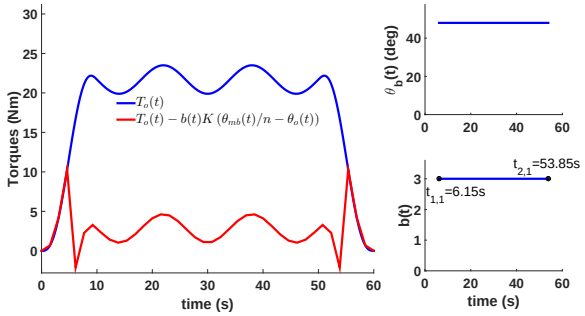

Fig. 4. Imposed torque on the output with the output blocked ($\theta_o = 0$). $\Delta t_a = \Delta t_r = 10s$, $\sigma_{max} = 50°$ and $K = 8.4$Nm/rad. The optimization shows that it is interesting to brake, with three motors, once between $t = [6.15; 53.85]$s with $\theta_{mb}/n = 50°$.

By defining the braking angles and times the trajectory of the motors is partially defined. Indeed one can notice on Fig. 4 that at $t = 6.15s$ three motors need to reach the position $\theta_m/n = \theta_{mb}/n = 50°$ (since the motors are all the same it does not matter which one) with a velocity equal to zero. Once it is done the brake can be used and will hold the three motors in this position until $t = 53.85$s.

B. Control strategy of the DC motors

The optimization to find the control set of the DC motors is a set of small optimal control problems divided into parts were no motors are braking and parts where several motors

are braking (thus their trajectory is completely defined) and the other motors need to provide the remaining torque. The first optimization problem can be defined as:

$$\begin{cases} J_m\ddot{\theta}_{mi} + \left(\nu + \frac{K_m^2}{R}\right)\dot{\theta}_{mi} = \frac{K_m}{R}U_i - \frac{C_G}{n}K\left(\theta_{mi}/n - \theta_o\right) \\ \min\limits_{U_i} J_2 = \int_{t_{2,j-1}}^{t_{1,j}} \left(\sum_{i=1}^{p} U_i\left(U_i - K_m\dot{\theta}_{mi}/n\right)/R\right) dt \\ \sum_{i=1}^{p} K\left(\theta_{mi}/n - \theta_o\right) = T_o \\ \theta_{mi}\left(t_{1,j}\right) = \theta_{mb}\left(t_{1,j}\right) \quad i = 1, ..., b\left(t_{1,j}\right) \\ \dot{\theta}_{mi}\left(t_{1,j}\right) = 0 \quad i = 1, ..., b\left(t_{1,j}\right) \\ \theta_{mi}\left(t_{1,j}\right) = \text{Free} \quad i = b\left(t_{1,j}\right)+1, ..., p \\ \dot{\theta}_{mi}\left(t_{1,j}\right) = \text{Free} \quad i = b\left(t_{1,j}\right)+1, ..., p \\ |I_i| \le I_{max} \quad |U| \le U_{max} \\ |\theta_{mi}/n - \theta_o| \le \sigma_{max} \quad |\dot{\theta}_{mi}| \le \dot{\theta}_{max} \end{cases} \tag{7}$$

For $j = 1$ we have $t_{2,0} = t_0$ and thus the initial conditions of the optimization problem are the initial conditions of the system. The goal of the optimization problem is to find the control set U such that J_2 (the energy consumed) is minimized. The final conditions ensure that the motors supposed to brake reach the angles θ_{mb} (with zero velocity) found in the optimization problem of section V-A. The end-points of the motors that are not braking remain free. There are also inequality constraints ensuring that the voltages, currents, velocities of the motors and deformation of the springs remain within acceptable limits. This optimization is used, for the task defined on Fig. 4, for $t = [0; 6.15]$s and $t = [53.85; 60]$s. For $t = [53.85; 60]$s the final conditions are also the final conditions of the system.
The second optimization problem is given by:

$$\begin{cases} J_m\ddot{\theta}_{mi} + \left(\nu + \frac{K_m^2}{R}\right)\dot{\theta}_{mi} = \frac{K_m}{R}U_i - \frac{C_G}{n}K\left(\theta_{mi}/n - \theta_o\right) \\ \min\limits_{U_i} J_{2,1} = \int_{t_{1,j}}^{t_{2,j}} \left(\sum_{i=b(t_{1,j})+1}^{p} U_i\left(U_i - K_m\dot{\theta}_{mi}/n\right)/R\right) dt \\ \sum_{i=b(t_{1,j})+1}^{p} K\left(\theta_{mi}/n - \theta_o\right) = T_o - bK\left(\theta_{mb}(t)/n - \theta_o(t)\right) \\ \theta_{mi}\left(t_{2,j}\right) = \text{Free} \quad i = b\left(t_{1,j}\right)+1, ..., p \\ \dot{\theta}_{mi}\left(t_{1,j}\right) = \text{Free} \quad i = b\left(t_{1,j}\right)+1, ..., p \\ |I_i| \le I_{max} \quad |U| \le U_{max} \\ |\theta_{mi}/n - \theta_o| \le \sigma_{max} \quad |\dot{\theta}_{mi}| \le \dot{\theta}_{max} \end{cases} \tag{8}$$

This optimization thus only concerns the non-braking motors. One can notice that the constraint linking the loads on the motors has been modified to account for the passive contribution of the units braking ($T_o - bK\left(\theta_{mb}(t)/n - \theta_o(t)\right)$). The terminal conditions of the problem remain free and the initial conditions are simply the positions of the motors found by solving equation (7). Similarly, the initial conditions of equation (7), when solved several times, are found by solving equation (8). The results are depicted on Fig. 5. The optimal control problem has been solved using GPOPS-II [15].

VI. EXPERIMENTAL RESULTS

As discussed in Section III-C, the blocked output experiment performed on the +SPEA compares the effect of two different sets of motor and brake commands. The objective is twofold:

- Ensure the model described in Section V is correct.
- Verify that the devised control strategy reduces the overall energy consumption.

In the first experiment, all brakes are disabled. As such, the system works as if 4 SEAs are driving a single output. Moreover, as shown in Fig. 5, the motor commands for all 4 motors are equal. In the second experiment, the brakes can be enabled at will. If a brake is enabled, its power consumption drops to zero while a certain output torque is provided. The desired output trajectory is shown in black in Fig. 5. The trajectory starts and ends at 0 Nm and oscillates several times around 21 Nm. The model and control strategy described in Section V are then used to calculate the required motor and brake commands in time, in order to ensure this output trajectory is followed by all motor units in parallel, both for the experiments with brakes disabled and with brakes enabled. The motor commands are sent directly to the motors and closed-loop controlled via the motor encoders. The output torque is measured, but not used for closed-loop control. As shown in the measurements of Fig. 5, both experiments approximate the modeled output torque for clearly different motor and brake commands.

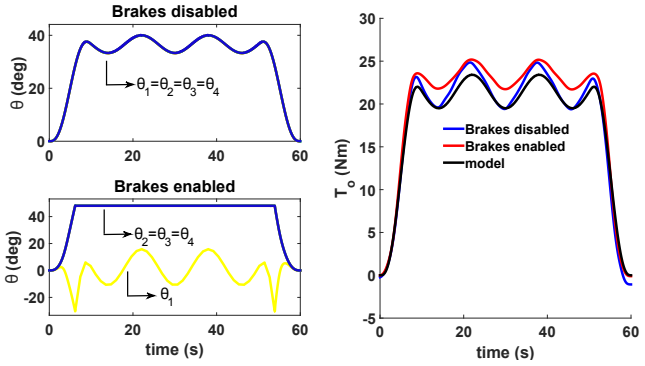

Fig. 5. Two different sets of motor and brake commands (left), results in two output trajectories that approximate the modeled oscillating reference output torque (right).

The difference in motor and brake commands results in a difference in motor current. The motor current in Fig. 6 (left) of motor 1 for both experiments (brakes disabled and brakes enabled) clearly shows a reduction in motor current for the experiments where the brakes are enabled on the one hand, and a good match between model and measurement on the other hand. The motor current for the motors where the brakes are activated drops to 0 A as indicated in Fig. 6 (right). Moreover, the average I_1 is also lower when the brakes are enabled. For clarity reasons, only the modeled motor current of motor 2 I_2 is plotted, and shows a good match with the experiments.

The electric power P of each motor in time, in Fig. 7 (left), is clearly lower for the experiment where the brakes are enabled compared to where the brakes are disabled. As a result, the electric energy required by all motors in total is more than a factor 4 lower when the brakes are enabled. Finally, it can be observed that the measurements follow the same trend as the model.

VII. CONCLUSIONS AND FUTURE WORK

A. Conclusions

In this work we introduced the +SPEA actuation schematic and presented the first prototype. A +SPEA actuator is

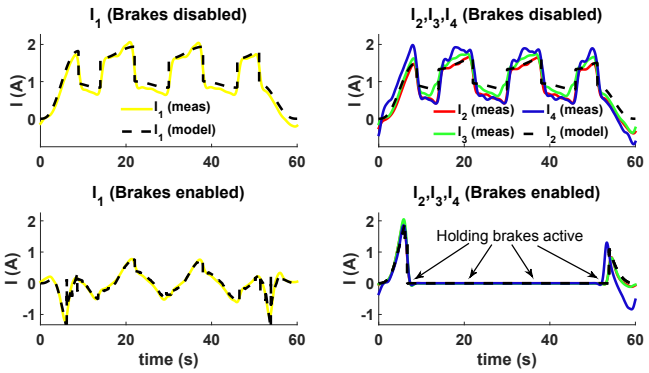

Fig. 6. The motor current model shows a clear fit with the experiments. The effect of the holding brakes is clear: the motor current drops to 0 A.

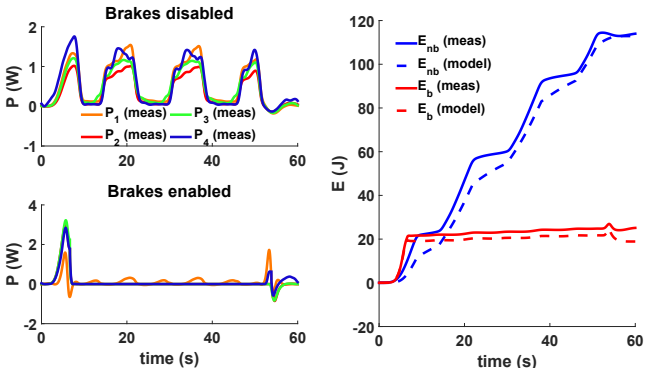

Fig. 7. The energy consumption of the +SPEA when the brakes are enabled is more than a factor 4 lower than when the brakes are disabled.

characterized by several motor units of SEAs, where a locking mechanism is added in every unit. A first control strategy is presented which deploys the inherent redundancy and virtues of the brakes in order to minimize the energy consumption for a certain task. The experiments show a clear difference in energy consumption by the total of the motors, while the output performance is similar.

B. Future work

The current experiments are performed with blocked output where the output torque is measured. In future experiments, a load side motor will be added in order to track output experiments with desired output torque and position. As such, an enriched set of profiles related to specific robotic applications (e.g. pick and place robots, exoskeletons, etc.) can be compared. The holding brakes will be replaced by passive non-backdrivable mechanisms in the next +SPEA, and modularity will be introduced to the motor units. Concerning control, a complete optimal controller will be designed instead of the current controller that solely generates the optimal output position trajectories. Finally, the use of springs with varying stiffness and different motor types in a single +SPEA will be studied.

ACKNOWLEDGMENT

This work was supported in part by the ERC-grant SPEAR (no.337596). Tom Verstraten and Glenn Mathijssen are funded by PhD Fellowship of the Research Foundation - Flanders (FWO). The authors would like to thank Michiel Plooij for his help on the GPOPS simulations, Tom van der Hoeven for his help in brainstorm sessions, and Merle Braatz for her help on the mechanical design.

REFERENCES

[1] G. A. Pratt and M. M. Williamson, “Series elastic actuators,” in *IEEE/RSJ International Conference on Intelligent Robots and Systems (IROS)*, vol. 1, 1995, pp. 399–406.

[2] B. Vanderborght, A. Albu-Schaeffer, A. Bicchi, E. Burdet, D. Caldwell, R. Carloni, M. Catalano, O. Eiberger, W. Friedl, G. Ganesh, *et al.*, “Variable impedance actuators: A review,” *Robotics and Autonomous Systems*, vol. 61, no. 12, pp. 1601–1614, 2013.

[3] U. Mettin, P. X. La Hera, L. B. Freidovich, and A. S. Shiriaev, “Parallel elastic actuators as a control tool for preplanned trajectories of underactuated mechanical systems,” *The international journal of robotics research*, vol. 29, no. 9, pp. 1186–1198, 2010.

[4] M. Holgate and T. G. Sugar, “Active compliant parallel mechanisms,” in *ASME 2014 International Design Engineering Technical Conferences and Computers and Information in Engineering Conference*. American Society of Mechanical Engineers, 2014, pp. 1–7.

[5] S. K. Au, J. Weber, and H. Herr, “Powered ankle–foot prosthesis improves walking metabolic economy,” *IEEE Transactions on Robotics*, vol. 25, no. 1, pp. 51–66, 2009.

[6] M. Cempini, M. Fumagalli, N. Vitiello, and S. Stramigioli, “A clutch mechanism for switching between position and stiffness control of a variable stiffness actuator,” in *Robotics and Automation (ICRA), 2015 IEEE International Conference on*, May 2015, pp. 1017–1022.

[7] M. Plooij, G. Mathijssen, P. Cherelle, D. Lefeber, and B. Vanderborght, “Lock your robot: A review of locking devices in robotics,” *Robotics Automation Magazine, IEEE*, vol. 22, no. 1, pp. 106–117, March 2015.

[8] E. J. Rouse, L. M. Mooney, and H. M. Herr, “Clutchable series-elastic actuator: Implications for prosthetic knee design,” *The International Journal of Robotics Research*, pp. 1–6, 2014.

[9] D. F. B. Haeufle, M. D. Taylor, S. Schmitt, and H. Geyer, “A clutched parallel elastic actuator concept: Towards energy efficient powered legs in prosthetics and robotics,” in *IEEE RAS EMBS International Conference on Biomedical Robotics and Biomechatronics (BioRob)*, 2012, pp. 1614–1619.

[10] N. Tsagarakis, S. Morfey, H. Dallali, G. Medrano-Cerda, and D. Caldwell, “An asymmetric compliant antagonistic joint design for high performance mobility,” in *IEEE/RSJ International Conference on Intelligent Robots and Systems (IROS)*, Nov 2013, pp. 5512–5517.

[11] G. Mathijssen, D. Lefeber, and B. Vanderborght, “Variable recruitment of parallel elastic elements: Series-parallel elastic actuators (spea) with dephased mutilated gears,” *IEEE/ASME Trans. Mechatron.*, 2014, (Accepted).

[12] G. Mathijssen, R. Furnemont, S. Beckers, T. Verstraten, D. Lefeber, and B. Vanderborght, “Cylindrical cam mechanism for unlimited subsequent spring recruitment in series-parallel elastic actuators,” in *IEEE International Conference on Robotics and Automation (ICRA)*, 2015.

[13] G. Mathijssen, J. Schultz, B. Vanderborght, and A. Bicchi, “A muscle-like recruitment actuator with modular redundant actuation units for soft robotics,” *Robotics and Autonomous Systems*, 2015.

[14] T. Verstraten, G. Mathijssen, R. Furnémont, B. Vanderborght, and D. Lefeber, “Modeling and design of geared dc motors for energy efficiency: Comparison between theory and experiments,” *Mechatronics*, 2015.

[15] M. A. Patterson and A. V. Rao, “Gpops-ii: A matlab software for solving multiple-phase optimal control problems using hp-adaptive gaussian quadrature collocation methods and sparse nonlinear programming,” *ACM Transactions on Mathematical Software (TOMS)*, vol. 41, no. 1, p. 1, 2014.